Assessment against DNS data of a coupled CFD-stochastic model for particle dispersion in turbulent channel flows

A. Dehbi

Paul Scherrer Institut
Department of Nuclear Energy and Safety
Laboratory for Thermal-hydraulics
5232 Villigen, Switzerland
abdel.dehbi@psi.ch

Abstract

The accurate prediction of particle transport is a primary safety issue. Tracking particles in Lagrangian fashion can naturally be performed with CFD tools which provide the right framework to follow the paths of particles in complex geometries. The presence of turbulent structures in the fluid complicates the particle tracking problem considerably, because particle trajectories are no longer deterministic and additional modeling of the velocity fluctuations is needed. In the present investigation, a Lagrangian continuous random walk (CRW) model is developed to predict turbulent particle dispersion in wall-bounded flows with prevailing inhomogeneous turbulence. The particle model uses 3D mean flow data from the Fluent CFD code, as well as Eulerian statistics from Direct Numerical Simulation (DNS) databases. The turbulent fluid velocities are based on the non-dimensional Langevin equation.

The model predictions are compared to the DNS data by Marchioli et al. (2007) who produced detailed statistics of velocity and transfer rates for classes of particles having Stokes numbers between 0.2 and 125 and dispersed in a parallel channel flow with Re_τ=150. The model is in very good agreement with the DNS data for the various measures of particle dispersion. The predicted deposition rates are also in good agreement with the widely used experimental correlation of McCoy and Hanratty (1977) and Liu and Agarwal (1974).

1. INTRODUCTION

During operating conditions in nuclear power plants, droplet-laden vapor flows are common (feedwater heaters, steam lines, etc), and droplet impingement on pipe walls is thought to be the main contributor to flow assisted corrosion (FAC) (Ferng and Horng, 2008), a mechanism which has led to small breaches many times in the past years. Steam generators also produce droplets which can damage turbine blades if they are not caught upstream in the piping (Katolickya et al., 2007). In hypothetical severe reactor accidents, particle-laden gas mixtures flow in the primary piping as well as in the containment. The accurate prediction of particle transport and deposition is therefore a primary safety issue. Tracking particles in Lagrangian fashion can naturally be performed with CFD tools which provide the right framework to follow the paths of particles in complex geometries. The interaction between the various forces acting on the particles (drag, gravity, lift, thermophoresis, etc) can harmoniously be addressed, in stark contrast to lumped parameter safety codes which add velocities due to different mechanisms, an incorrect procedure in general.

The presence of turbulent structures in the fluid complicates the particle tracking problem considerably, because particle trajectories are no longer deterministic and additional modeling of the fluid velocity fluctuations is needed.

Many methods have been developed to take into account velocity fluctuations in the turbulent flow. In principle, the simplest and more “physical” method is Direct Numerical Simulation (DNS) (McLaughlin, 1989) in which turbulence is “reproduced” by solving the transient Navier-Stokes continuity and momentum equations on a sufficiently fine grid and with a sufficiently small time step.

In such a way, all relevant spatial and temporal scaled are resolved. Large-Eddy Simulations (LES) (Wang and Squires, 1997) are conceptually similar to DNS, except that the computational effort is reduced somewhat by requiring the grid to be only so fine as to resolve the largest eddies, whereas the smaller, quasi isotropic eddies are modeled. While being widely used, DNS-LES/LPT methods remain computationally expensive, and their extension to general geometries poses very tough and sometimes intractable computational challenges.

An alternative method, which borrows from the family of stochastic models, attempts to simulate turbulence using complementary equations whereby the instantaneous turbulent velocities are calculated from local quantities such as the mean turbulent kinetic energy, the Eulerian time scale and the distance to the wall. Examples of these treatments are random walk models which have been popular due to their relative ease of implementation and reasonable computational expense. In Discrete Random Walk (DRW) models (Gosman and Ioannides, 1983), the turbulent dispersion of particles is modeled as a succession of interactions between a particle and eddies which have finite lengths and lifetimes. In wall-bounded flows, the original isotropic DRW model of Gosman & Ioannides (1983) has been improved to account for anisotropic turbulence in the near-wall regions. This improved DRW model has been used with some success to predict turbulent particle deposition in isothermal 2D channels (Kallio and Reeks, 1989), in general 3D isothermal flows (Dehbi, 2007) or in cooled pipes (Kröger and Drossinos, 2000).

Continuous Random Walk (CRW) models provide a more physically sound picture of fluid turbulence, as they represent the instantaneous velocities in a continuous way. CRW models, which are usually based on the Langevin equation, have been shown to provide more realistic predictions of turbulent particle dispersion than DRW, in particular in flows where inhomogeneous effects are important such as mixing layers (MacInnes and Bracco, 1992) or free shear flows (Bocksell and Loth, 2001). Hence a CRW model will be adopted in this investigation.

One of the main goals of this investigation is to describe turbulent particle dispersion in general wall-bounded geometries. Mean flow parameters in complex turbulent flows can only be predicted on a routine basis using standard Computational Fluid Dynamics (CFD) tools based on the Reynolds Averaged Navier Stokes (RANS) equations. Ideally then, turbulent particle dispersion in general 3D geometries could be done by coupling CFD with reliable particle dispersion models in a single application. However, as shown recently by Tian and Ahmadi (2007), the use e.g. of DRW in combination with the state-of-the-art anisotropic Reynolds Stress Model (RSM) still led to large overpredictions of particle deposition rates in 2D parallel ducts. This is due to the fact that the RSM calculated root mean square (rms) of the normal velocity near the wall overpredicts the profiles determined by DNS studies, and no grid refinement can remedy this problem. Using the same RSM-DRW framework, Parker et al. (2007) were able to obtain dimensionless deposition velocities that overestimated the experimental data by less than one order of magnitude, which is the best that can be achieved with today's CFD codes in their default mode. Better results were however obtained when Tian and Ahmadi (2007) combined the use of RSM for the mean flow field, the Langevin equation for the turbulent fluctuations, and a DNS-supplied correlation for the normal velocity rms close to the wall.

Based on the above, it becomes clear that quantitatively accurate predictions of turbulent particle dispersion can only be achieved through a substantial improvement in the treatment of particle-turbulence interactions in the boundary layer. This treatment needs to be developed and incorporated in the CFD tools in order to properly account for near-wall effects which control to a large extent the physics of particle deposition. In this investigation, the fluid fluctuations will be computed from a Langevin equation based model, which will be combined with the mean flow data obtained from the Fluent 6.3 code (Fluent, 2006). Fluent 6.3 is a state of the art code based on finite volume methods that provides a wide choice of turbulence models (k-ε, k-ω, RSM, etc). The necessary Eulerian statistics to close the Lagrangian particle tracking model will be supplied by the available DNS databases of channel flows. The model predictions are compared to the extensive DNS database provided by Marchioli et al. (2007) who produced detailed statistics of velocity and transfer rates for 6

classes of particles having Stokes numbers of 0.2 to 125 and dispersed in a parallel channel flow with Re_τ=150.

2. PARTICLE FORCE BALANCE

A spherical particle is assumed to be entrained in a wall-bounded turbulent flow in isothermal conditions. The only forces acting on the particle are taken to be drag and gravity. Brownian diffusion is neglected since the simulated particles will have geometric diameters greater than 0.2 μm. The lift force is also ignored as a first approximation in order to concentrate on the effect of turbulence on thermophoretic deposition. The vector force balance on a spherical particle is written as follows:

$$\frac{dU_p}{dt} = F_D(U - U_p) + g(1 - \frac{\rho_f}{\rho_p}) \qquad (1)$$

where the drag force per unit mass may be expressed as:

$$F_D = \frac{18\mu}{\rho_p d_p^2} C_D \frac{\mathrm{Re}_p}{24} \qquad (2)$$

In the above, U is the fluid velocity, U_p is the particle velocity, ρ_p the particle density, ρ_f the fluid density, g the gravity acceleration vector, d_p the particle geometric diameter, μ the fluid molecular viscosity, and Re_p the particle Reynolds number defined as:

$$\mathrm{Re}_p = \frac{d_p \left| U - U_p \right|}{\nu} \qquad (3)$$

ν being the fluid kinematic viscosity. The drag coefficient is computed in the Fluent code from the following equation:

$$C_D = \beta_1 + \frac{\beta_2}{\mathrm{Re}_p} + \frac{\beta_3}{\mathrm{Re}_p^2} \qquad (4)$$

where the β's are constants which apply to spherical particles for wide ranges of Re_p.

$$U_p = \frac{dx}{dt} \qquad (5)$$

In laminar flows, the expressions (1) to (5) are sufficient to compute the trajectory of individual particles. The particle deposition rates and concentration profiles are found in a determinist way, and the procedure was shown by Healy et al. (2001) to yield accurate predictions of particle dispersion. When turbulent fluctuations exist in the fluid flow, the computation of particle dispersion is no longer deterministic and the particle dispersion problem becomes more complicated to handle. To determine the mean dispersion statistics of particles, it is necessary to perform many trajectory computations. The stochastic modeling of the fluid velocity fluctuations is discussed in the next section.

3. THE NORMALIZED LANGEVIN EQUATIONS

In the following section, we present the Langevin equations defining the fluctuating velocity field along a particle track. The domain is assumed to be wall-bounded, so that it can be subdivided in two regions: the boundary layer region with strongly anisotropic turbulence, and a bulk region where the

turbulence is assumed approximately isotropic but generally inhomogeneous. Since the model is meant to handle both the boundary layer as well as the isotropic bulk regions, the Langevin equations will take different forms depending on the location of the particle.

3.1 The normalized Langevin equation in boundary layers

In the Langevin equation, the incremental change in the turbulent fluid velocity seen by an inertial particle is assumed to be comprised of three terms: a damping term which is proportional to the turbulent velocity, a stochastic forcing term that has zero mean, and a mean drift correction term that ensures the well-mixed criterion for tracer particles in inhomogeneous fields (Legg and Raupach, 1982). To improve the predictive abilities of the Langevin equation in boundary layers, further modifications were put forth. Durbin (1983, 1984) and Thompson (1984), extending the ideas of Wilson et al. (1981), proposed that the Langevin equation be normalized to account for strongly inhomogeneous turbulence. Following Iliopoulos et al. (2003), the normalized Langevin equation in the boundary layer along the i^{th} coordinate is written as:

$$d\left(\frac{u_i}{\sigma_i}\right) = -\left(\frac{u_i}{\sigma_i}\right)\cdot\frac{dt}{\tau_L} + d\eta_i + A_i dt \qquad (6)$$

In the above, u_i is the fluid fluctuating velocity component, σ_i the rms of velocity $\sqrt{\overline{u_i^2}}$, τ_L a Lagrangian time scale to be defined in Section 4, $d\eta_i$ a succession of uncorrelated random forcing terms, and A_i the mean drift correction term. The forcing moments can, to a first order, be expressed as:

$$\overline{d\eta_i d\eta_j} = \frac{\overline{u_i u_j}}{\sigma_i \sigma_j}\left[\frac{2}{\tau_L}\right]\cdot dt \qquad (7)$$

where overbar in the above expression means time averages. Equation (7) is obtained assuming jointly Gaussian distributions for the random forcing terms η_i (Mito and Hanratty, 2002). Bocksell and Loth (2006) showed that the normalized drift correction term A_i along the path of a particle with arbitrary inertia can be expressed as follows:

$$A_i = u_j\,\overline{\frac{\partial\left(\frac{u_i}{\sigma_i}\right)}{\partial x_j}}\cdot\frac{1}{1+Stk} = \frac{\partial\left(\frac{\overline{u_j u_i}}{\sigma_i}\right)}{\partial x_j}\cdot\frac{1}{1+Stk} \qquad (8)$$

where the Einstein convention of summing up over repeated indices is followed. In the above, the particle Stokes number *Stk* is defined as:

$$Stk = \frac{\tau_p}{\tau_L} \qquad (9)$$

where τ_p is the particle relaxation time defined according to the local particle Reynolds number:

$$\tau_p = \frac{C_c \rho_p d_p^2}{18\mu} \qquad \mathrm{Re_p} \le 1 \qquad (10)$$

and:

$$\tau_p = \frac{4}{3}\frac{\rho_p}{\rho_f}\frac{C_c d_p^2}{C_D\left|U - U_p\right|} \qquad \mathrm{Re_p} > 1 \qquad (11)$$

C_c is the Cunningham correction slip factor which is nearly 1 for particles with diameters above 1 μm. For the evaluation of A_i, and in compliance with the boundary layer approximation, we concentrate on the derivatives in the wall normal direction and ignore the cross terms. Hence:

$$A_i = \frac{\partial\left(\frac{\overline{u_2 u_i}}{\sigma_i}\right)}{\partial x_2}\cdot\frac{1}{1+Stk} \qquad (12)$$

where the subscripts 1, 2 and 3 stand for streamwise, wall-normal and spanwise directions, respectively.

The mean drift correction term A_i is very important to include in order to avoid the unphysical migration of small inertia particles towards the boundary layer. Thomson (1987) demonstrated that taking into account the drift correction A_i fulfills the so-called well-mixed criterion, that is, the requirement that very low inertia particles (tracers) that are initially well mixed in the isothermal inhomogeneous turbulent flow will remain well mixed with time. Mito and Hanratty (2002) later verified this feature in their simulations of fluid particles originating from uniformly distributed sources in channel flow boundary layers. Following Mito and Hanratty (2004), A_1 and A_3 are set to zero. The latter approximation should not have a large impact on the predictions because particle deposition is largely controlled by wall-normal fluctuations.

Based on the preceding formulations and assumptions, one can then write the normalized Langevin equations as follows for the streamwise, normal, and spanwise directions of the boundary layer:

$$d\left(\frac{u_1}{\sigma_1}\right) = -\left(\frac{u_1}{\sigma_1}\right)\cdot\frac{dt}{\tau_L} + \sqrt{\frac{2}{\tau_L}}\cdot d\xi_1 \qquad (13)$$

$$d\left(\frac{u_2}{\sigma_2}\right) = -\left(\frac{u_2}{\sigma_2}\right)\cdot\frac{dt}{\tau_L} + \sqrt{\frac{2}{\tau_L}}\cdot d\xi_2 + \frac{\partial\sigma_2}{\partial x_2}\cdot\frac{dt}{1+Stk} \qquad (14)$$

$$d\left(\frac{u_3}{\sigma_3}\right) = -\left(\frac{u_3}{\sigma_3}\right)\cdot\frac{dt}{\tau_L} + \sqrt{\frac{2}{\tau_L}}\cdot d\xi_3 \qquad (15)$$

where the $d\xi_i$'s are Gaussian random numbers with zero mean and variance dt.

3.2 The normalized Langevin equation in the isotropic bulk

In the bulk region (here for $y^+>100$) turbulence is taken to be isotropic, although not necessarily homogeneous. The Langevin equations become simpler in that region, and Dehbi (2008) showed that they can be expressed as:

$$d\left(\frac{u_1}{\sigma}\right) = -\left(\frac{u_1}{\sigma}\right)\cdot\frac{dt}{\tau_L} + \sqrt{\frac{2}{\tau_L}}\cdot d\xi_1 + \frac{1}{3\sigma}\cdot\frac{\partial k}{\partial x_1}\cdot\frac{dt}{1+Stk} \qquad (16)$$

$$d(\frac{u_2}{\sigma}) = -(\frac{u_2}{\sigma}) \cdot \frac{dt}{\tau_L} + \sqrt{\frac{2}{\tau_L}} \cdot d\xi_2 + \frac{1}{3\sigma} \cdot \frac{\partial k}{\partial x_2} \cdot \frac{dt}{1+Stk} \quad (17)$$

$$d(\frac{u_3}{\sigma}) = -(\frac{u_3}{\sigma}) \cdot \frac{dt}{\tau_L} + \sqrt{\frac{2}{\tau_L}} \cdot d\xi_3 + \frac{1}{3\sigma} \cdot \frac{\partial k}{\partial x_3} \cdot \frac{dt}{1+Stk} \quad (18)$$

where σ is the rms of the isotropic velocity field, and k the turbulent kinetic energy. The equations (13) through (15) and (16) through (18) describe possible changes along a particle path of the turbulent fluid velocities in the boundary layer and bulk region, respectively. The integration of these equations in time is done using the first order implicit Euler method, and the dynamic time step is taken to be min (10^{-6}s, 0.1 τ_p), which was shown to be small enough not to influence the results. The integration of the Langevin equations necessitates Eulerian statistics to close the problem. This is addressed in the next section.

4. SPECIFICATION OF THE EULERIAN STATISTICS AND TIMESCALES

The Eulerian rms of velocity are obtained from fits of the DNS data obtained by Marchioli et al. (2007). The fits are shown in Figure 1, are given by:

$$\sigma_1^+ \equiv \frac{\sigma_1}{u^*} = \frac{A1 + C1 \cdot y^+ + E1 \cdot y^{+2} + G1 \cdot y^{+3} + I1 \cdot y^{+4}}{1 + B1 \cdot y^+ + D1 \cdot y^{+2} + F1 \cdot y^{+3} + H1 \cdot y^{+4} + J1 \cdot y^{+5}} \quad (19)$$

$$\sigma_2^+ \equiv \frac{\sigma_2}{u^*} = \frac{A2 + C2 \cdot y^+ + E2 \cdot y^{+2} + G2 \cdot y^{+3} + I2 \cdot y^{+4}}{1 + B2 \cdot y^+ + D2 \cdot y^{+2} + F2 \cdot y^{+3} + H2 \cdot y^{+4} + J2 \cdot y^{+5}} \quad (20)$$

$$\sigma_3^+ \equiv \frac{\sigma_3}{u^*} = \frac{A3 + C3 \cdot y^+ + E3 \cdot y^{+2} + G3 \cdot y^{+3}}{1 + B3 \cdot y^+ + D3 \cdot y^{+2} + F3 \cdot y^{+3}} \quad (21)$$

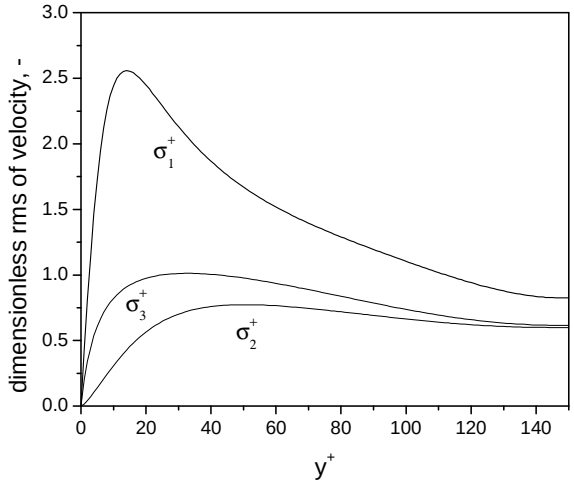

Figure 1: Rms fits of the DNS data by Marchioli et al. (2007)

y+ is the wall distance in dimensionless units defined as:

$$y^+ = \frac{y u^*}{\nu} \quad (22)$$

y is the particle distance to the nearest wall, u* the friction velocity derived from the local wall shear stress τ_w and wall fluid density $\rho_{f,w}$ as follows:

$$u^* = \sqrt{\frac{\tau_w}{\rho_f}} \qquad (23)$$

Researcher usually estimate the Lagrangian time scales τ_L by tracking fluid particles in DNS simulations, and subsequently computing the Lagrangian autocorrelations. By going through this procedure, Bocksell and Loth (2006) have determined that the Lagrangian time scales in all directions are reasonably well approximated by the fits obtained by Kallio and Reeks (1989):

$$\tau_L^+ = 10 \qquad y^+ \leq 5 \qquad (24)$$

$$\tau_L^+ = 7.122 + 0.5731 \cdot y^+ - 0.00129 \cdot y^{+2} \qquad 5 \leq y^+ \leq 100 \qquad (25)$$

where:

$$\tau_L = \tau_L^+ \cdot \frac{\nu}{(u^*)^2} \qquad (26)$$

In the isotropic bulk flow, taken here to be the region where y+ > 100, the Lagrangian time scale can be estimated from the local turbulent kinetic energy k and dissipation rate ε :

$$\tau_L = \frac{2}{C_o} \cdot \frac{k}{\varepsilon} \qquad (27)$$

Mito and Hanratty (2002) have found that a value of 14 for C_o provided fair agreement with the time scales computed from their DNS database. Hence this value will used in equation (27) to estimate τ_L in the bulk.

5. COUPLING THE LANGEVIN MODEL TO THE FLUENT CFD CODE

While the integration of the Langevin equations in the bulk region poses no particular problem in general geometries, care must be exercised when the particle is in the boundary layer, because one must correctly assign the Eulerian rms values in a local body-fitted coordinates system which varies with particle location. The algorithm to do so is explained at length by Dehbi (2008).

The Fluent CFD code (Fluent, 2006) provides the mean flow parameters as well as a module to integrate the particle equations of motion. The Langevin model described earlier was implemented in Fluent as a User Defined Function (UDF) subroutine which supplies the trajectory calculation module with the fluctuating fluid velocity seen by a particle at each time step. Details of the coupling between the Fluent CFD code and the stochastic Langevin model are also provided by Dehbi (2008).

6. RESULTS AND DISCUSSION

In a previous study by Dehbi (2008), the Langevin model described here was assessed against isothermal particle deposition data in various geometries and found to be quite accurate in predicting the deposition rates. In this investigation, the model predictions are compared to the DNS data of particle dispersion produced by Marchioli et al. (2007).

In that investigation particles are dispersed in a fully developed turbulent flow of air. The fluid flows between two infinite parallel walls. The periodic channel simulating the infinite parallel walls channel has a half-height h of 0.02 m, a width of 2πh and a length of 4πh. The density of air is taken to be 1.3 kg/m^3 and its kinematic viscosity 15.7 x 10^{-6} m^{2}s^{-1}. Periodic boundary conditions are enforced in the axial and spanwise directions. The axial fluid velocity is 1.65 m/s, with a corresponding friction velocity u* of 0.11775 m/s. The Reynolds number based on the axial velocity is thus 2100, whereas that based on friction velocity is 150.

Marchioli et al. (2007) studied the effects of inertia, gravity and the lift force on particle velocity statistics and transfer rates. In the present investigations, and for the sake of conciseness , we restrict ourselves to the effect of inertia. For all the simulations, the CFD Best Practice Guidelines (ERCOFTAC, 2000) were followed to ensure that particle deposition results were grid-independent. These Best Practice Guidelines include in particular:

- Use of hexahedral meshes.
- Use of 2 different grid resolutions.
- Adequate resolution of the boundary layer, with 50 cells within the boundary layer (y+ < 100).
- Centroid of the wall-nearest cell has a y+ of order 1.
- Second order accuracy for the discretization equations.

In addition, since the geometries are relatively simple, the k-ε model for turbulence is chosen for all simulations and is expected to give reasonably accurate predictions of the mean flow.

For the specification of particle inertia, the dimensionless relaxation time τ^+ is defined as:

$$\tau^+ = \frac{\tau_p u^{*2}}{\nu} \qquad (28)$$

The dimensionless tracking time is normalized as follows:

$$t^+ = \frac{t \cdot u^{*2}}{\nu} \qquad (29)$$

where t is the physical time in second. The particles are tracked for a period of time t^+= 1200, which is the longest tracking time in the DNS tracking simulations. This corresponds to the time taken by a fluid particle to travel about 9 times the channel length.

6.1 Particle concentration profiles

The particle concentration profiles are studied in this section in order to better understand the interactions between turbulence and particle inertia. Four classes of particles having relaxation times τ+ of 0.2, 5, 25 and 125 are considered. These correspond to geometric diameters of 9.12 μm, 45.6 μm, 102 μm, and 228 μm, respectively. In each simulation, 50 000 particles are injected uniformly from the inlet face. Experimentation with largest samples showed virtually no difference in the results. Once a particle center is at a distance less than the radius of the particle, the latter is considered to have hit the wall, and is reflected back to the domain, as in the computations by Marchioli et al.. At an instant t, the tracks are frozen, and the volumetric particle distribution profile is determined. To do so, the volume of the channel is subdivided in N_b wall parallel bins along the height of the channel. The bins are thinner near the wall and become progressively wider as one moves towards the center of the channel, according to the following formula for the bth bin thickness used by Marchioli et al. (2007):

$$\Delta y_b^+ = \frac{\mathrm{Re}_\tau}{2}\left(1-\cos(\pi\cdot\frac{b-1}{N_b-1})\right) \qquad (30)$$

where the Reynolds number based on the friction velocity is 150, and N_b is 51. The purpose of such grading is to resolve well the laminar and buffer layers near le wall (y+ of 30), which are the regions where anisotropic effects are the strongest. To compute the particle concentration profile, one simply counts the airborne particles in each bin, and then normalizes this number with the volume of the bin as well as the total number of particles. The normalized particle concentrations shown in Figure 2 for dimensionless times of t^+=675 and 1125, corresponding respectively to the average time taken by a fluid particle to travel 5.74 and 8.71 times the length of the channel. The DNS results of Marchioli et al. (2007) are shown for comparison. The results can be summarized are followed:

- The Langevin model predictions are in excellent agreement with the DNS results, both in terms of trends and magnitudes.
- Particles with very low inertia (τ^+=0.2) tend to remain approximately well mixed in the channel regardless of the time spent.
- Particles with medium and high inertia develop substantial concentration peaks well inside the laminar layer. These peaks increase as time evolves, indicating that steady state concentrations have not yet been reached even after about 110 channel heights. This is consistent with previous DNS computations (Marchioli et. al, 2007, Picciotto, 2005) which have highlighted the very long distance required before particles concentrations reach fully developed conditions.
- The largest peaks are recorded for mid-range inertia particles (τ^+=25). These particles are thus the most affected by turbulence. Particles with the highest inertia (τ^+=125) display smaller peaks because their motion is more decoupled from the fluid fluctuations.

6.2 Mean axial velocity profiles

The mean axial fluid velocity computed by the Fluent CFD code and the DNS computation are first compared in Figure 3. can be seen, the two profiles are close to one another in the laminar sublayer, but the CFD profile displays a slight deficit in the middle of the channel. In the DNS computations, there were only slight differences between the particle axial velocities and the fluid velocity. Hence to capture these slight differences, the particle axial velocities will subsequently be compared to the CFD fluid profile rather than the DNS one.

The particle velocity profiles are computed in a way identical to that followed by Marchioli et al. (2007): at selected time steps, one determines the bin containing the particle, then the instantaneous mean velocity for that bin is computed, and in a third step, these mean velocities are averaged over time for a prescribed sample of time steps from t^+=742 to t^+=1192. The selected number of time steps is 450, so that one samples every 1 dimensionless unit of time. The mean axial velocity of the particles profiles are shown in Figure 4.

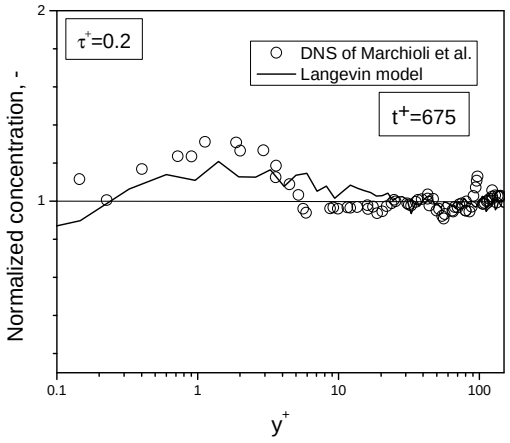
τ+=0.2
DNS of Marchioli et al.
Langevin model
t+=675
Normalized concentration, -
y+

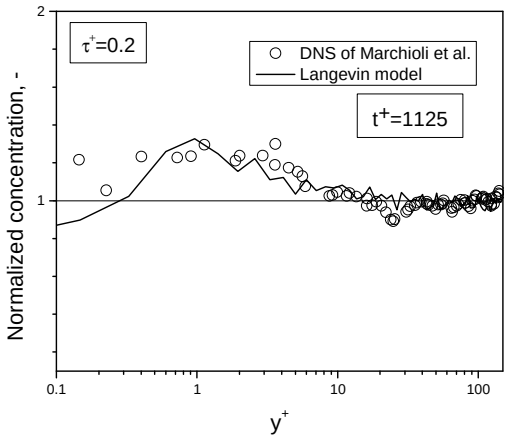
τ+=0.2
DNS of Marchioli et al.
Langevin model
t+=1125
Normalized concentration, -
y+

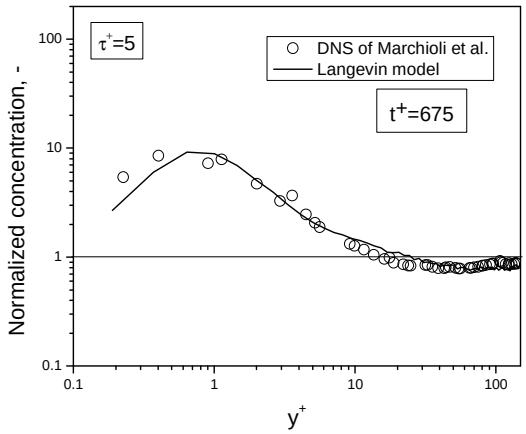
τ+=5
DNS of Marchioli et al.
Langevin model
t+=675
Normalized concentration, -
y+

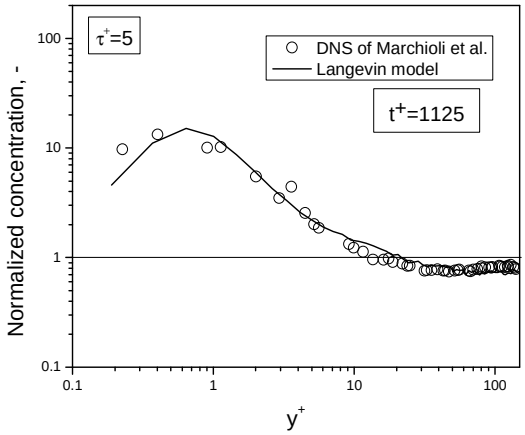
τ+=5
DNS of Marchioli et al.
Langevin model
t+=1125
Normalized concentration, -
y+

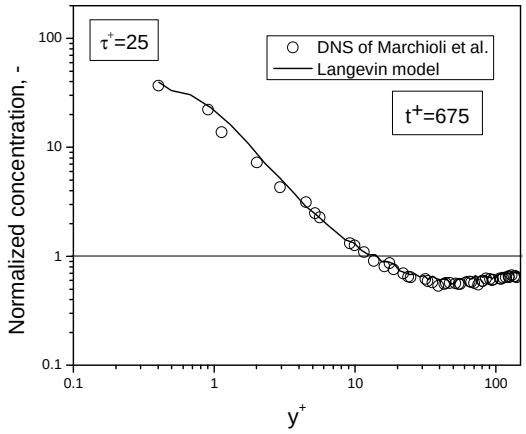
τ+=25
DNS of Marchioli et al.
Langevin model
t+=675
Normalized concentration, -
y+

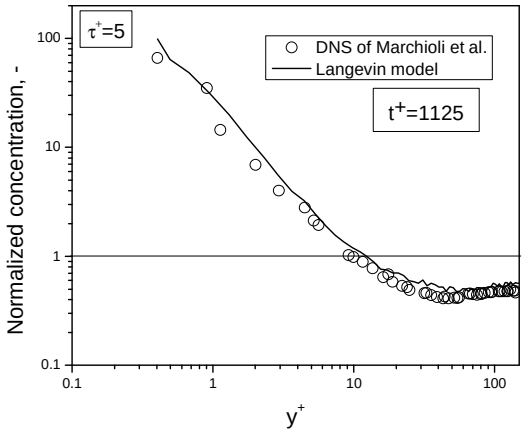
τ+=5
DNS of Marchioli et al.
Langevin model
t+=1125
Normalized concentration, -
y+

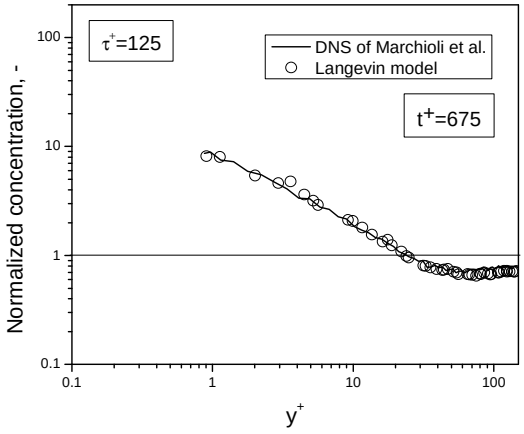
τ+=125
DNS of Marchioli et al.
Langevin model
t+=675
Normalized concentration, -
y+

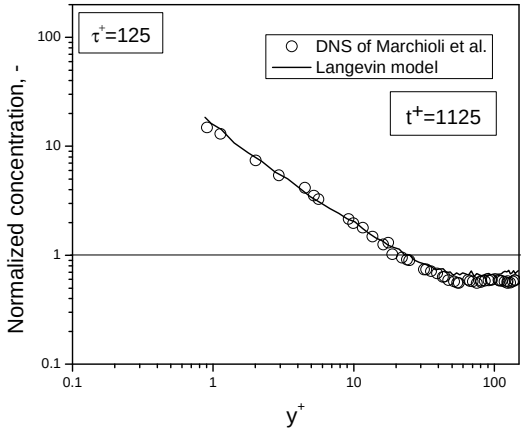
τ+=125
DNS of Marchioli et al.
Langevin model
t+=1125
Normalized concentration, -
y+

Figure 2: Concentration profiles as a function of time and particle inertia

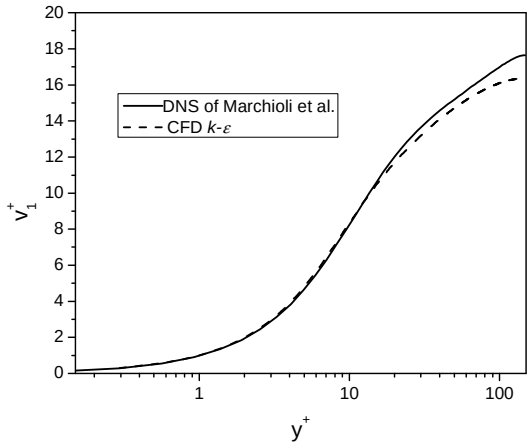

Figure 3: mean axial velocity: DNS vs CFD

For particles up to a τ^+=25, the axial mean velocity profile is essentially identical to the fluid profile. For τ^+=125, the particles lag the fluid in the laminar sublayer, but are slightly faster then the fluid in the logarithmic region. Both of these trends are consistent with the Marchioli et al. findings.

6.3 Mean wall normal velocity profiles

The mean wall normal velocities predicted by the model are displayed in Figure 5 and compared to DNS profiles. For τ^+=0.02 the wall normal velocity is essentially at noise levels, which the Langevin model predicts well. For higher inertia, the Langevin model and DNS profiles are comparable. One notes however a slight overestimation of the magnitude of velocity as the particle inertia increases.

6.4 Rms of axial velocity

The rms values for the axial velocity in each bin are obtained from the 450 instantaneous mean velocities as well as the mean velocity in the time frame between t^+=742 and t^+=1192. Results are displayed in Figure 6 the axial velocity. The Langevin profiles are quite close to the DNS profiles, with a slight overprediction as particle inertia increases.

6.5 Rms of wall normal velocity

Results for the rms of the wall normal component of velocity are displayed in Figure 7 the wall normal velocity. As in the last section, the Langevin model predictions are in quite good agreement with the DNS data, with a small overprediction as particle inertia increases.

6.6 Particle deposition rates compared to experimental data

The model prediction of deposition rates is presented in this section. A hypothetical channel of height 0.01 m, length L 0.8 m, and width 0.1 m is considered. A uniform velocity of 11 m/s is imposed on the inlet face (Re= 7500 based on channel height), while atmospheric pressure boundary conditions are assigned at the outlet face. The lateral faces consist of symmetry planes, so that the mean flow is essentially two dimensional. The mean flow is computed using the standard k-ε model with enhanced wall treatment. Particles are injected uniformly along a line joining the two walls in the middle of the

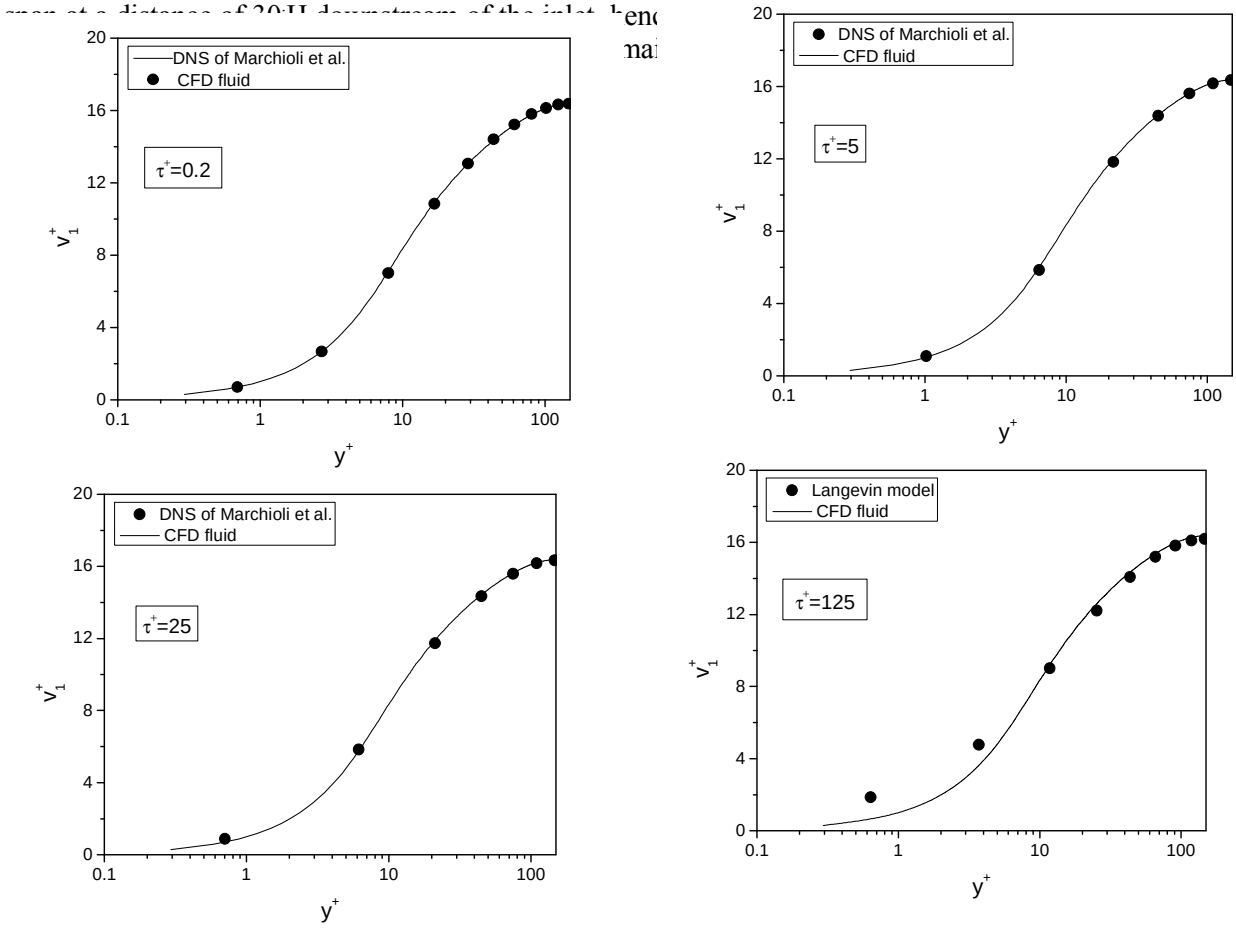

Figure 4: Mean streamline velocity as a function of particle inertia

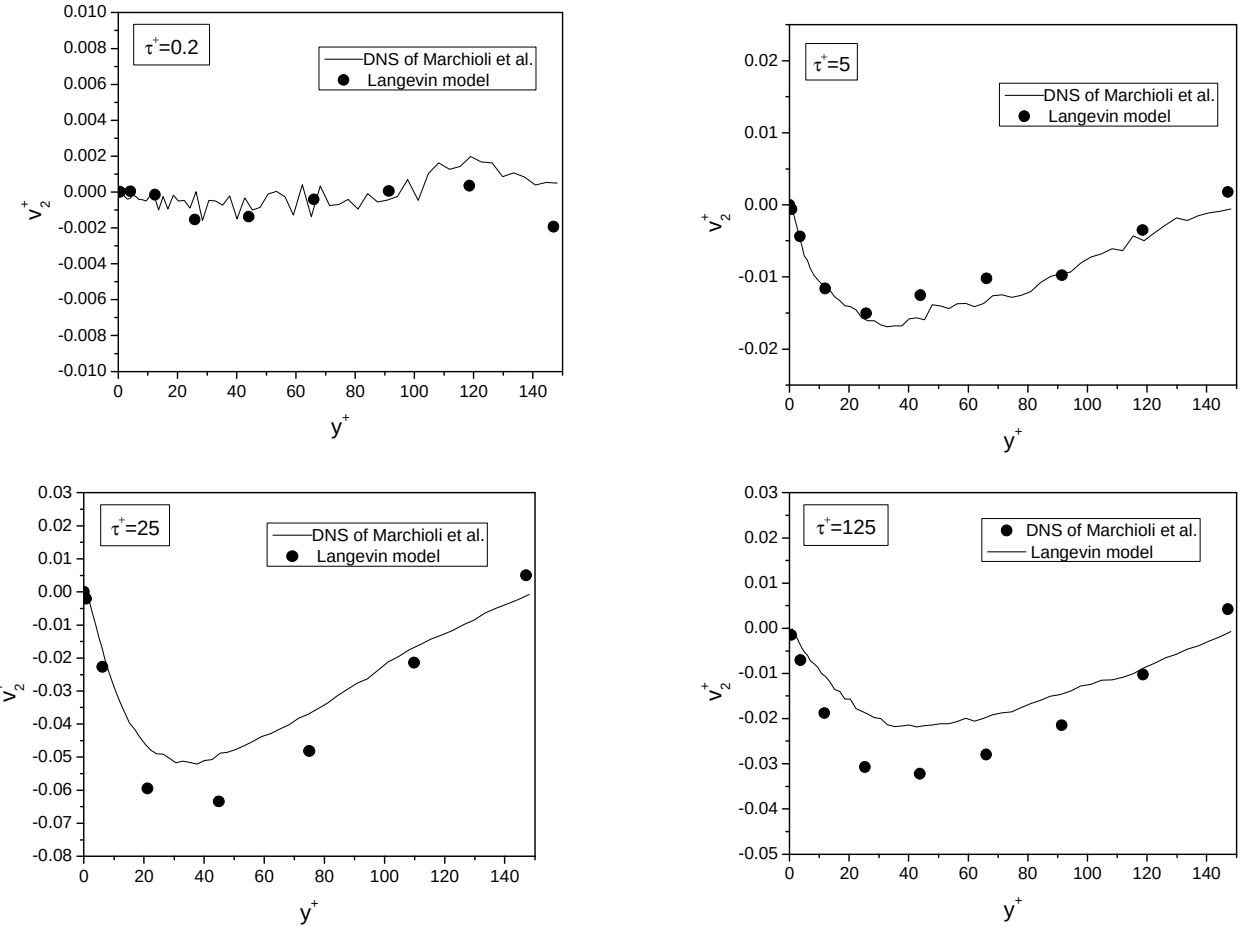

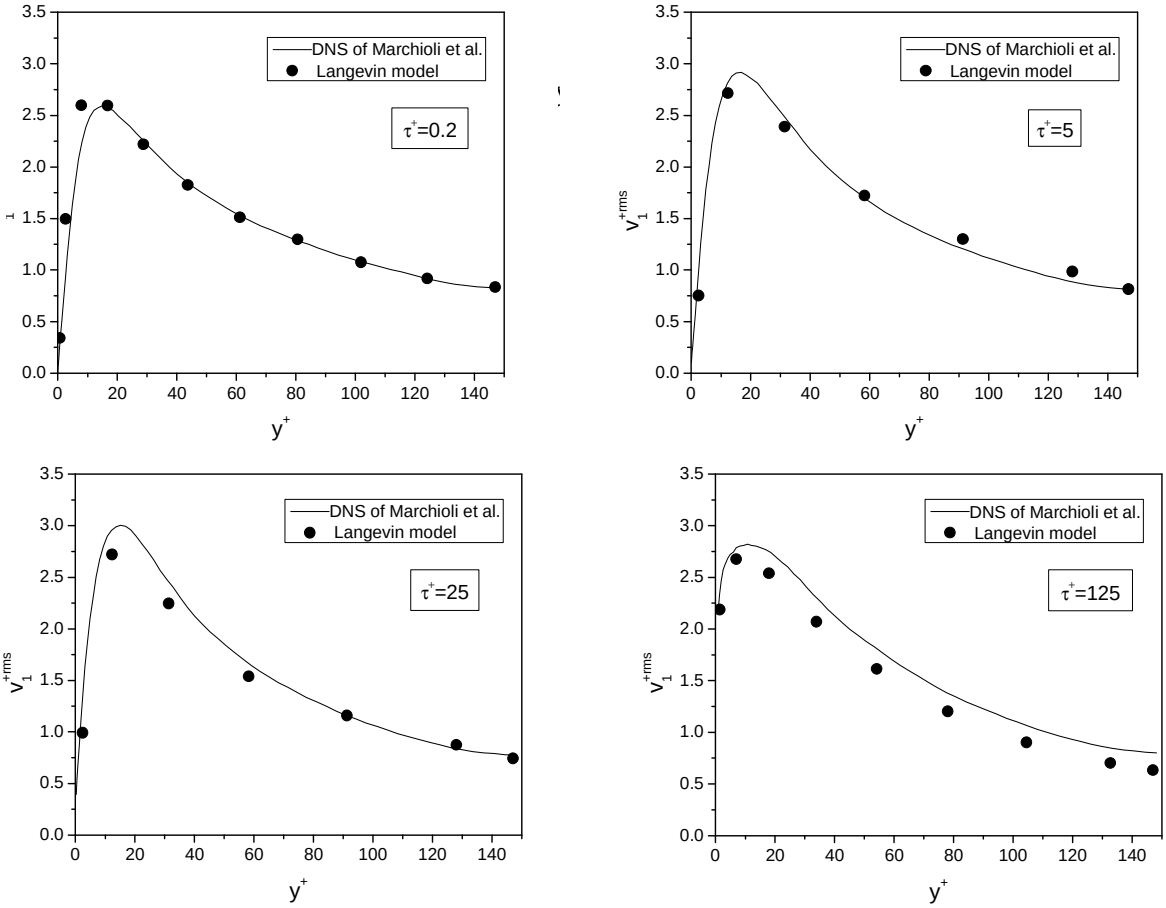

Figure 6: rms of streamwise velocity as a function particle inertia

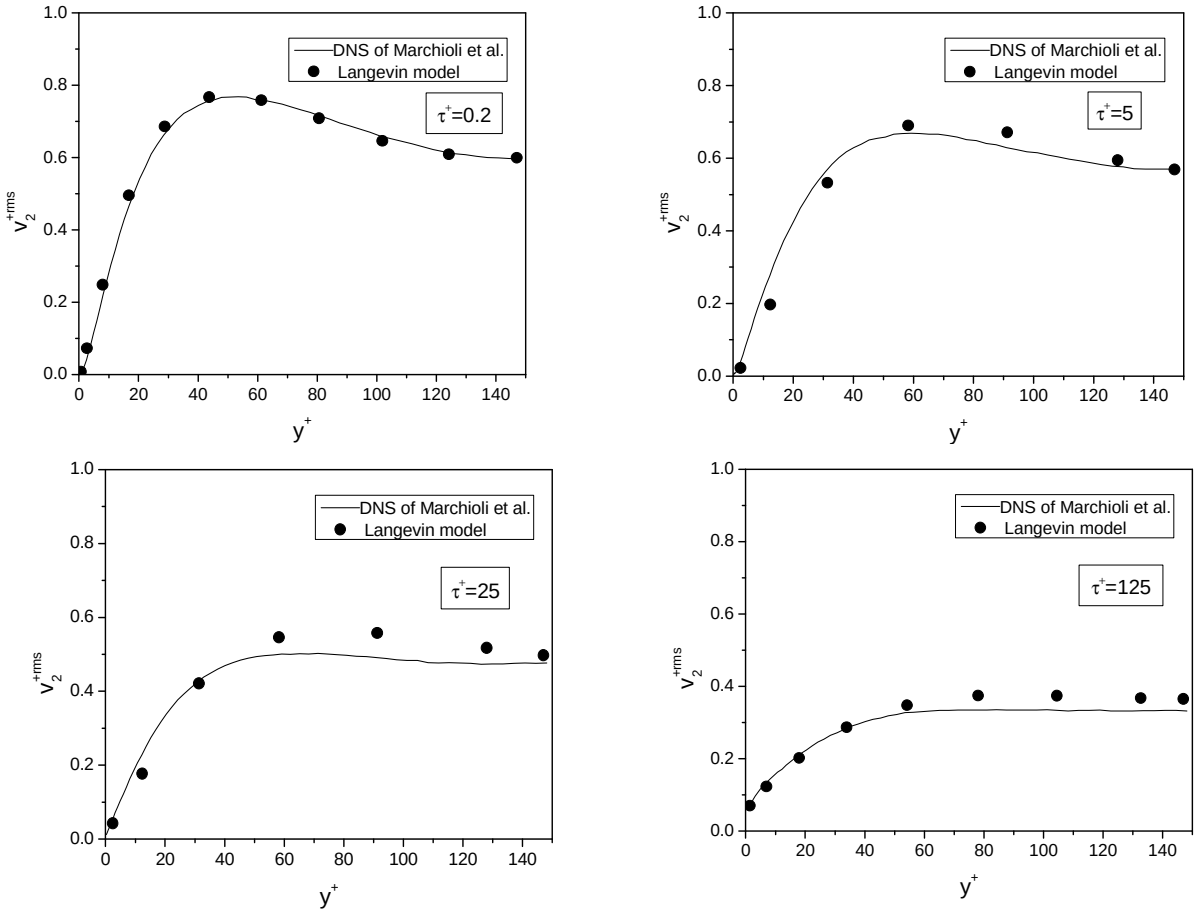

Figure 7: rms of wall normal velocity as a function particle inertia

The particle deposition in the channel is recorded for 10 000 unit density particles, a number found to be sufficiently large to provide stationary statistics. The deposition velocity is compared to the widely used fits of McCoy and Hanratty (1977) and Liu and Agarwal (1974) given by:

$$V_{MH}^{+} = \max\ (0.000325 \cdot (\tau^{+})^{2}, 17) \tag{31}$$

$$V_{LA}^{+} = \max\ (0.0006 \cdot (\tau^{+})^{2}, 0.1) \tag{32}$$

where the dimensionless deposition velocity is defined as:

$$V^{+} = \frac{1}{2}\frac{H}{L}\frac{U}{u^{*}}\ln(\frac{C_{in}}{C_{out}}) \tag{33}$$

In the above U is the mean velocity, H is the channel height, L the length of the channel section where deposition is studied, and C_{in} and C_{out} refer to the particle number concentrations entering and leaving the section, respectively. Accordingly, the deposited fraction in a length L is given by:

$$\eta = 1 - \exp\left(-2\frac{L}{H}\frac{u^{*}}{U}V^{+}\right) \tag{34}$$

Deposition results are shown in Figure 8 As can be seen, the agreement between the model and the experimental fit is good and certainly well within the data scatter band of the correlations. One notes however an underprediction of the data in the very low deposition velocity region, which is probably due to the non-inclusion of the lift force.

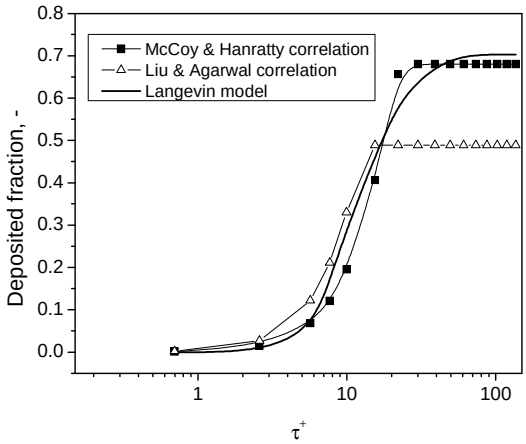

Figure 8: Deposited fraction: comparison with experimental correlations

7. CONCLUSIONS

A Lagrangian continuous random walk (CRW) model is developed to predict particle dispersion in arbitrary wall-bounded geometries with prevailing anisotropic, inhomogeneous turbulence. The particle tracking model relies on 3D mean flow data provided by the Fluent CFD code, as well as Eulerian statistics computed from DNS databases. The time history of the fluctuating fluid velocities is obtained from the normalized Langevin equation which takes into account turbulence inhomogeneities. The model incorporates a drift velocity correction for arbitrary inertia particles. The model predictions using the k–ε model for the mean flow are compared to the DNS data by Marchioli et al. (2007) who produced detailed statistics of velocity and transfer rates for 4 classes of particles having Stokes numbers of 0.2 to 125 and dispersed in a parallel channel flow with Re_{τ}=150. The model is in very good agreement with the DNS data for the various measures of dispersion parameters, i.e:

instantaneous particle concentration profiles and mean and rms profiles of streamwise and wall-normal particle velocities. The model reproduces well-known results such as the clustering of particles in the boundary layer, as well as the gradual de-correlation between particles and turbulence with increasing inertia. In addition, the "well-mixed" criterion is achieved such that tracer particles retain approximately uniform concentrations when introduced uniformly in the domain, and their deposition velocity is vanishingly small, as it should be. Particle deposition rates are also in good agreement with the widely used experimental correlation of McCoy and Hanratty (1977) and Liu and Agarwal (1974).

This overall excellent agreement of the CFD-Langevin model with the extensive DNS database as well as empirical correlations for particle deposition rates gives confidence that accurate simulations of particle dispersion in practical turbulent flows is within reach with today's CFD tools.

Acknowledgements

The author wishes to express his gratitude to Professor C. Marchioli of the University of Udine for making available his DNS data base, and for extensive interactions during this work.

REFERENCES

Bockell T.L., Loth, E., 2001. Random walk models for particle diffusion in free shear flows. AIAA J., 39, 1086-1096.

Bockell T.L., Loth E., 2006. Stochastic modeling of particle diffusion in a turbulent boundary layer. International Journal of Multiphase Flow, 32, 1234-1253.

Dehbi, A., 2007. A CFD model for particle dispersion in turbulent boundary layer flows, Nuclear Engineering and Design, doi:10.1016/j.nucengdes.2007.02.055. In Press.

Dehbi, A., 2008. Turbulent particle dispersion in arbitrary wall-bounded geometries: a coupled CFD-Langevin-equation based approach. International Journal of Multiphase Flow. doi: 10.1016/j.ijmultiphaseflow.2008.03.001

Durbin, P.A., 1983. Stochastic differential equations and turbulent dispersion, NASA Reference Publication 1103.

Durbin, P.A.,1984. Comments on the papers by Wilson et al. (1981) and Legg and Raupach (1982). Boundary Layer Meteorology 29, 409-411.

ERCOFTAC, 2000. European Research Community on Flow Turbulence and Combustion (ERCOFTAC) Best Practice Guidelines, Version 1.

Ferng Y.-M., Horng, C.-T., 2007. Prediction of possible wear sites on the shell wall of feedwater heater due to droplet impingement using CFD models. Nuclear Engineering and Design 237, 1560-1568

Fluent, 2006. Fluent 6.3 Users Guide, Lebanon, USA.

Gosman, A.D., Ioannides, E., 1983. Aspects of computer simulation of liquid fuelled combustors. Journal of Energy 7, 482–490.

Healy, D.P., Young, J.B., 2001. Calculation of inertial particle transport using the Osiptsov Lagrangian method. 4th International Conference on Multiphase Flow, New Orleans, Paper DJ4.

Iliopoulos I., Mito Y., Hanratty T.J., 2003. A stochastic model for solid particle dispersion in a nonhomogeneous turbulent field. International Journal of Multiphase Flow 29, 375–394.

Kallio, G.A., Reeks, M.W., 1989. A numerical simulation of particle deposition in turbulent boundary layers. International Journal of Multiphase Flow 3, 433-446.

Kröger C., Drossinos Y., 2000. A random-walk simulation of thermophoretic particle deposition in a turbulent boundary layer. International Journal of Multiphase Flow 26, 1325-1350.

Katolickya, J., Jichaa M. and Maresb R., 2007. Droplets deposition in steam piping connecting steam generator and steam turbine in nuclear plant. Nuclear Engineering and Design 237, 1534-1549.

Legg B.J., Raupach, M.R. 1982. Markov-chain simulation of particle dispersion in inhomogeneous flows: The mean drift velocity induced by a gradient in Eulerian velocity variance. Boundary Layer Meteorology 24, 3–13.

Liu, B.Y.H., Agarwal, J.K. 1974. Experimental observation of aerosol deposition in turbulent flow. Aerosol Science 5, 145–155.

MacInnes, J.M., Bracco, F.V., 1992. Stochastic particle dispersion modeling and the tracer particle limit. Physics of Fluids A 4, 2809–2824.

Marchioli, C., Picciotto M., Soldati A., 2007. Influence of gravity and lift on particle velocity statistics and transfer rates in turbulent vertical channel flow. International Journal of Multiphase Flow 33, 227-251.

McCoy D.D., Hanratty T.J., 1977. Rate of deposition of droplets in annular two-phase flow. International Journal of Multiphase Flow 3, 319-331.

McLaughlin, J. B., 1989. Aerosol particle deposition in numerically simulated channel flow. Physics of Fluids A 1, 1211-1224.

Mito Y., Hanratty T.J., 2002. Use of a modified Langevin equation to describe turbulent dispersion of fluid particles in a channel flow. Flow, Turbulence and Combustion, 68, 1-26.

Mito Y., Hanratty, T.J., 2004. A stochastic description of wall sources in a turbulent field: part 2. Calculation for a simplified model of horizontal annular flows. International Journal of Multiphase Flow 30, 803-825.

Parker S., Foat T., Preston S., (2007). Towards quantitative prediction of aerosol deposition from turbulent flows. Journal of Aerosol Science39, Pages 99-112.

Picciotto M., Marchioli C., Soldati A., 2005. Characterization of near-wall accumulation regions for inertial particles in turbulent boundary layers. Phys. Fluids 17, 98-101.

Thompson, D.J., 1984. Random walk modeling of dispersion in inhomogeneous turbulence. Quarterly Journal of the Royal Meteorological Society110,1107-1120.

Thompson, D.J., 1987. Criteria for the selection of stochastic models of particle trajectories in turbulent flows. Journal of Fluid Mechanics 180, 529-559.

Tian, T. Ahmadi, G., 2007. Particle deposition in turbulent duct flows—comparisons of different model predictions. Journal of Aerosol Science,38,, 377-397

Wang, Q., Squires, K.D., 1997. Large eddy simulation of particle deposition in a vertical turbulent channel flow. International Journal of Multiphase Flow 22, 667–683.

Wilson, J.D., Thurtell, G.W., Kidd, G.E. 1981. Numerical simulation of particle trajectories in inhomogeneous turbulence. Part 2: Systems with variable turbulent velocity scale. Boundary Layer Meteorology 21, 423-441.